Article

Hydrogen Storage in Boron Nitride and Carbon Nanomaterials

Takeo Oku

Department of Materials Science, The University of Shiga Prefecture, Hassaka 2500, Hikone,
Shiga 522-8533, Japan; E-Mail: oku@mat.usp.ac.jp; Tel.: +81-749-288-368; Fax: +81-749-288-590

Academic Editor: Enrico Sciubba

Abstract: Boron nitride (BN) nanomaterials were synthesized from LaB_6 and Pd/boron powder, and the hydrogen storage was investigated by differential thermogravimetric analysis, which showed possibility of hydrogen storage of 1–3 wt%. The hydrogen gas storage in BN and carbon (C) clusters was also investigated by molecular orbital calculations, which indicated possible hydrogen storage of 6.5 and 4.9 wt%, respectively. Chemisorption calculation was also carried out for $B_{24}N_{24}$ cluster with changing endohedral elements in BN cluster to compare the bonding energy at nitrogen and boron, which showed that Li is a suitable element for hydrogenation to the BN cluster. The BN cluster materials would store H_2 molecule easier than carbon fullerene materials, and its stability for high temperature would be good. Molecular dynamics calculations showed that a H_2 molecule remains stable in a C_{60} cage at 298 K and 0.1 MPa, and that pressures over 5 MPa are needed to store H_2 molecules in the C_{60} cage.

Keywords: nanostructure; boron nitride; carbon; hydrogen gas storage; hydrogenation; molecular orbital calculation

---

1. Introduction

Hydrogen is a carrier with high energy density, and forms only water and heat. On the other hand, fossil fuels generate toxic fuels, such as CO_x, NO_x and SO_x. Therefore, clean hydrogen energy is expected as substitute of fossil fuel in the 21st century, and gas storage ability more than 6.5 wt% is needed for car application according to the US Department of Energy. Although $LaNi_5H_6$ is already used as an H_2 gas storage materials, the ability is only 1 wt% because of the large atomic number of La and Ni [1]. On the other hand, fullerene-like materials, which consist of light elements, such as boron,

carbon and nitrogen, would store more H_2 gas compared to the metal hydrides. Various works have been reported on hydrogen storage ability of carbon nanotubes, fullerenes and nanomaterials [1]. It was reported that multi-walled carbon nanotubes could absorb hydrogen from 1 wt% up to 4.6 wt%. These results indicate carbon nanotubes might be a possible candidate of hydrogen storage materials although the evaluation of hydrogen storage measurements is necessary. Many studies on H_2 gas storage in carbon (C) nanomaterials have been reported [2–7]. Boron nitride (BN) nanomaterials are also expected in prospective application because they provide good stability at high temperatures with high electronic insulation in air [8]. Hydrogen storage in BN nanomaterials has also been studied recently [9–16]. It is difficult to absorb hydrogen by physisorption, both inside nanotubes and at the interstitial channels of nanotubes at room temperature, which is due to too weak bonding of physisorbed hydrogen to reach large storage at room temperature. Therefore, it is considered that chemisorption is a necessary requirement for hydrogen storage at room temperature. It was reported that chemisorption ratio observed at room temperature increases with increasing alkali/carbon rate. Therefore, if the energy of chemisorption can be lowered, hydrogen storage ability of carbon and BN nanotubes would be improved.

The purpose of the present study is twofold. The first is to prepare BN nanotubes, nanocapsules and nanocages, and to investigate hydrogen gas storage by thermogravimetry/differential thermogravimetric analysis (TG/DTA) and first principle calculation. LaB_6 and Pd were selected in order to take advantage of their catalytic effect to produce the BN nanomaterials. La has shown excellent catalytic properties for producing a large number of single-walled carbon nanotubes and enlarging their diameter, and Pd is also expected to act as a hydrogen storage material. Although gas storage of hydrogen and argon in carbon nanotubes has been reported, carbon nanotubes are oxidized at 600 °C in air. On the other hand, BN starts to be oxidized into boron oxide and nitrogen ~900 °C in air, which indicates excellent heat resistance compared to carbon materials for gas storage. The differences between BN and C nanomaterials are summarized as shown in Table 1. To understand the formation of BN nanostructures, high-resolution electron microscopy (HREM) were carried out, which are very powerful methods for atomic structure analysis [17,18]. For the BN nanomaterials, hydrogen gas storage measurements were carried out using TG/DTA.

Table 1. Differences between boron nitride (BN) and C nanomaterials.

Properties	BN	C
Structure	4-, 6-, 8-membered rings	5-, 6-, 7-membered rings
Oxidation resistance	~900°C	~600 °C
Electronic property	Insulator	Metal-semiconductor
Energy gap (eV)	~6	0–1.7
Band structure	Direct transition	Indirect transition

The second purpose of the present work is to investigate H_2 gas storage ability of BN and C fullerene-like materials by theoretical calculation. Although huge amount of calculation is required to calculate nanotubes, it is considered that H_2 molecules enter from the cap of nanotubes. Energy of chemisorption and stable hydrogen position inside the clusters were investigated as cap structures of nanotubes. Influence of endohedral element on H_2 gas storage ability of BN fullerene-like materials

was also investigated by theoretical calculations. Energy of chemisorption was investigated for cage clusters as a cap structure of nanotubes, and $B_{24}N_{24}$ clusters, reported by mass spectrometry [8,19], were selected for the storage material. Li, K and Na elements were also selected for the doping atoms because these elements are of high electropositive character. The present study will give us a guideline for hydrogenation of BN nanomaterials as hydrogen storage materials.

2. Experimental Procedures and Calculation Methods

Mixture powder compacts made of boron particles (99%, 40 mm, Nilaco Corp., Tokyo, Japan), LaB_6 particles (99%, 1 mm, Wako Pure Chemical Industries Ltd., Osaka, Japan) and Pd particles (99.5%, 0.1 mm, Nilaco Corp., Tokyo, Japan), with the size of 3 mm in height and 30 mm in diameter were produced by pressing powder at 10 MPa. The atomic ratios of metal (M) to boron (B) were in the range of 1:1–1:10. The green compacts were set on a copper mold in an electric-arc furnace, which was evacuated down to 2.0×10^{-3} Pa. After introducing a mixed gas of Ar 0.025 MPa and N_2 0.025 MPa, arc-melting was applied to the samples at an accelerating voltage of 200 V and an arc current of 125 A for 2 s. Arc-melting was performed with a vacuum arc-melting furnace (NEV-AD03, Nissin Giken, Saitama, Japan), and the white/gray BN nanomaterial powders were collected from surface of the bulk. Samples for HREM observation were prepared by dispersing the materials on holy carbon grids. HREM observation was performed with a 300 kV electron microscope (JEM-3000F, JEOL, Tokyo, Japan). To confirm the formation of BN fullerene materials, energy dispersive x-ray spectroscopy analysis was performed using the EDAX system with a probe size of ~10 nm. In order to measure hydrogen gas storage in BN nanomaterials, BN nanomaterials were extracted from the obtained powder by a supersonic dispersing method based on the Stokes equation using ethanol. The Stokes equation is expressed as follows:

$$v = d^2(\sigma - \rho)g/18\eta \ (h = vt; \ v: \text{sedimentation rate}) \tag{1}$$

where η is the viscosity of liquid; σ is the density of particles; ρ is the density of liquid; g is the gravitational acceleration; d is the diameter of particles; t is the subsidence time; and h is the height of liquid. Since there is a big difference in the size and density of the produced BN nanocapsules/nanotubes and other powders, it is believed that this method would be effective for separation of BN nanomaterials [20]. After separation of BN nanomaterials, hydrogen storage was measured by TG/DTA at temperatures in the range of 20–300 °C in H_2 atmosphere [21].

To search the optimized structure of $B_{99}N_{99}$ and $B_{36}N_{36}$ with H_2 molecules, semi-empirical molecular orbital calculations (parameterized model revision 3, PM3) were performed. The energies of $B_{36}N_{36}$ with H_2 molecules were calculated by first principle single point energy calculation using Gaussian. In the calculation, 3-21G was used as ground function with Hartree-Fock level. $B_{24}N_{24}$, $B_{36}N_{36}$, $B_{60}N_{60}$ and C_{60} were selected for cluster calculations. To investigate the optimized structures, semi-empirical molecular orbital calculations (parameterized model revision 5, PM5) were performed by using MOPAC. Eigenvector following (EF) method was used for geometry optimization, and charge is 0. The default self-consistent method was restricted Hartree-Fock (HF). Multi-electron configuration interaction (MECI) was used in order to prevent repulsion between electrons becoming

excessive. Chemisorption calculations of hydrogen atoms were performed for $B_{24}N_{24}$, $B_{36}N_{36}$ and C_{60} by PM5 calculations [22,23].

$M@B_{24}N_{24}$ (M@: element encaged in $B_{24}N_{24}$) was selected for cluster calculations. To investigate the optimized structures and the chemisorption calculations of hydrogen atoms, molecular orbital calculations were performed by using PM5 in MOPAC. The EF method was used for geometry optimization. The default self-consistent method was restricted as HF, and the MECI was used. In the calculation, chemisorption of hydrogen was performed on boron and nitrogen positions outside the cage [24]. Energy levels and densities of states (DOS) for $B_{24}N_{24}$ and $Li@B_{24}N_{24}$ were also calculated by the first principles calculation with discrete variational (DV)-Xα method.

Molecular dynamics calculations were carried out to confirm the stability of H_2 molecules into C_{60} at 298 K and 0.1 MPa [25]. Number, temperature, and pressure (NTP) ensembles were used in the calculation as follows: number of atoms (N), temperature (T) and pressure (P) are constant. Conditions of H_2 gas storage were also calculated. Number, temperature, and enthalpy (NPH) ensembles were used in the calculation as follows: number of atoms (N), pressure (P) and enthalpy (H) are constant. These molecular dynamics were calculated by organic potential.

3. Results and Discussion

3.1. Synthesis of Boron Nitride Nanomaterials

For some metals, formation enthalpies with boron ($H^{for}B$) and nitrogen ($H^{for}N$) are indicated in Figure 1a,b, respectively. The data were from theoretical calculations [8]. Difference of formation enthalpy ($H^{for}N-H^{for}B$) is also shown in Figure 1c. The difference of formation enthalpy ($H^{for}N-H^{for}B$) is very important for the formation of BN fullerene nanomaterials, because reactivity with nitrogen and boron is decided by this enthalpy. Basically, BN nanotubes are formed when rare earth metals are used as catalytic metals, such as Y, Zr, Nb, Hf, Ta, W and La. These elements have minus enthalpy, as shown in Figure 1c. It means that catalytic elements for synthesis of BN nanotubes should be selected from those with minus formation enthalpy ($H^{for}N-H^{for}B$). From the present guideline, Sc element could be a good catalytic element to form BN nanotubes. The detailed formation mechanism of the nanostructures with different metals should be investigated further.

A HREM image of a BN nanotube produced using LaB_6 powder is shown in Figure 2a. In Figure 2a, the diameter of the five-layered BN nanotube is changing from bottom to top, and amorphous patches are observed mostly at the top. Low magnification images of BN nanostructures were reported [17,20]. A HREM image of BN nanocage produced from LaB_6/B powder is shown in Figure 2b, which indicates square-like shape, and four-membered rings of BN exist at the corner of the cage. The BN nanocage has a network-like structure, whose atomic arrangement is basically consistent with the $B_{36}N_{36}$ cluster structure [8]. BN nanocapsules with Pd nanoparticles were also produced as shown in Figure 2c, and Pd nanoparticles were covered by a few BN layers. In order to confirm the formation of BN nanocapsules, EDX analysis was carried out, which showed the atomic ratio of B:N ≈ 1.

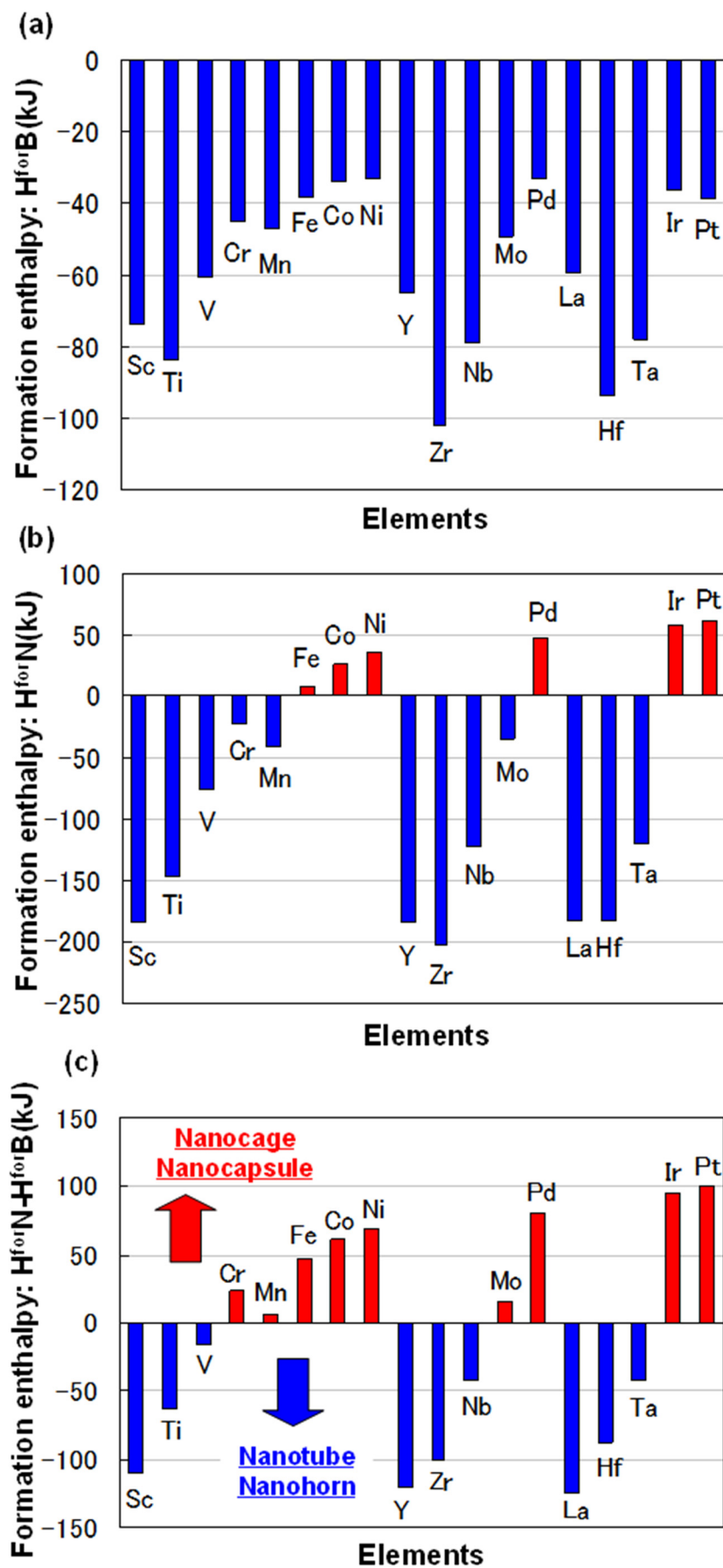**Figure 1.** (**a**) Formation enthalpy with boron ($H^{for}B$) and (**b**) nitrogen ($H^{for}N$); (**c**) difference of formation enthalpy ($H^{for}N$-$H^{for}B$).
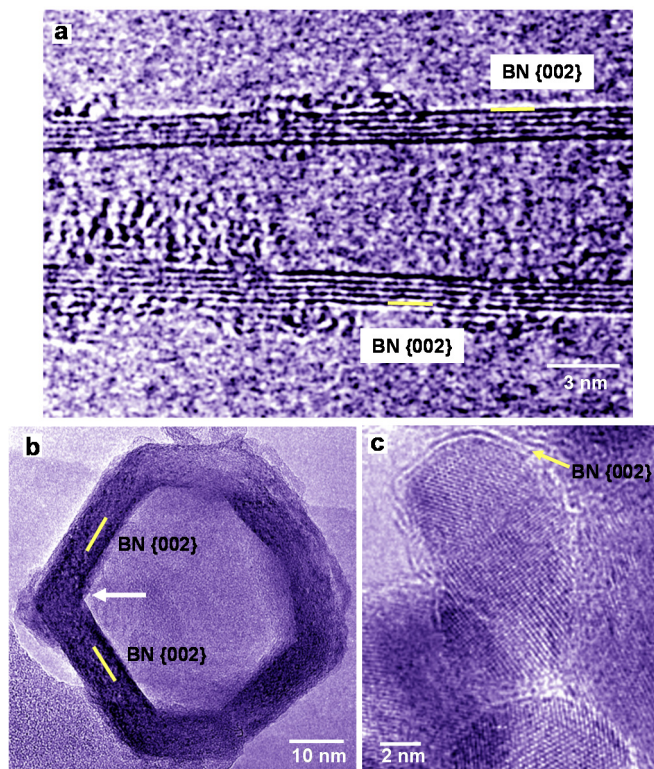
Figure 2. High-resolution electron microscopy (HREM) images of BN nanotube and BN nanocapsules produced using powder with ratios of: (**a**) La:B = 1:6; (**b**) La:B = 1:4; and (**c**) Pd:B = 1:4.

3.2. Hydrogen Storage in Boron Nitride Nanomaterials Studied by Thermogravimetry/Differential Thermogravimetric Analysis

DTA and TG curve of BN nanomaterials produced from LaB_6 powder is shown in Figure 3. At a temperature around 70 °C, an increase of sample weight of 0.3 mg is observed. Weight change for this sample was almost reversible, which indicates the reversibility of hydrogen adsorption. It also suggests that the hydrogen atoms would be physically absorbed. For the samples of La:B = 1:6 and Pd:B = 1:4, weight increases of 3.2% and 1.6% were observed, respectively, as listed in Table 2.
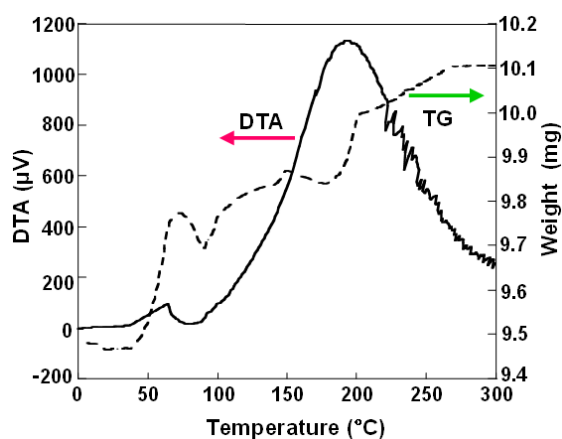

Figure 3. Differential thermogravimetric analysis (DTA) and thermogravimetry (TG) curve of BN nanocapsules and nanotubes produced using LaB_6 powder.

Table 2. Atomic ratio of starting materials, produced structures and hydrogen storage.

M:B	Nanostructures	Weight change (wt%)
La:B = 1:6	Nanotubes and nanocages	+3.2
La:B = 1:10	Nanotubes	+0.58
Pd:B = 1:4	Nanocapsules	+1.6

BN nanostructures would have energy barriers for H_2 molecules to pass through tetragonal and hexagonal rings. Figure 4 are structure models in which H_2 molecule passes from hexagonal rings of $B_{99}N_{99}$ and $B_{36}N_{36}$. Single point energies were calculated with changing set point of H_2 molecule from the center of the cage at intervals of 0.1 nm. There is energy barrier that is given for H_2 molecules to pass through the hexagonal rings. The energy barrier of $B_{36}N_{36}$ hexagonal rings showed the smallest value of 14 eV in the present calculation, which is smaller than that of 27 eV at tetragonal rings. The DE of C_{60} hexagonal rings was also calculated to be 16 eV for comparison. This value is higher than that of $B_{36}N_{36}$ hexagonal rings, and the H_2 molecule would pass from hexagonal rings of $B_{36}N_{36}$ easier than from hexagonal rings of C_{60}. It is known that H_2 molecules are adsorbed on walls of single-walled carbon nanotubes over 7 MPa as an experimental result. As a result of the comparison, H_2 molecules enter into $B_{36}N_{36}$ from hexagonal rings easier than tetragonal rings $B_{36}N_{36}$ and hexagonal rings of C_{60}.
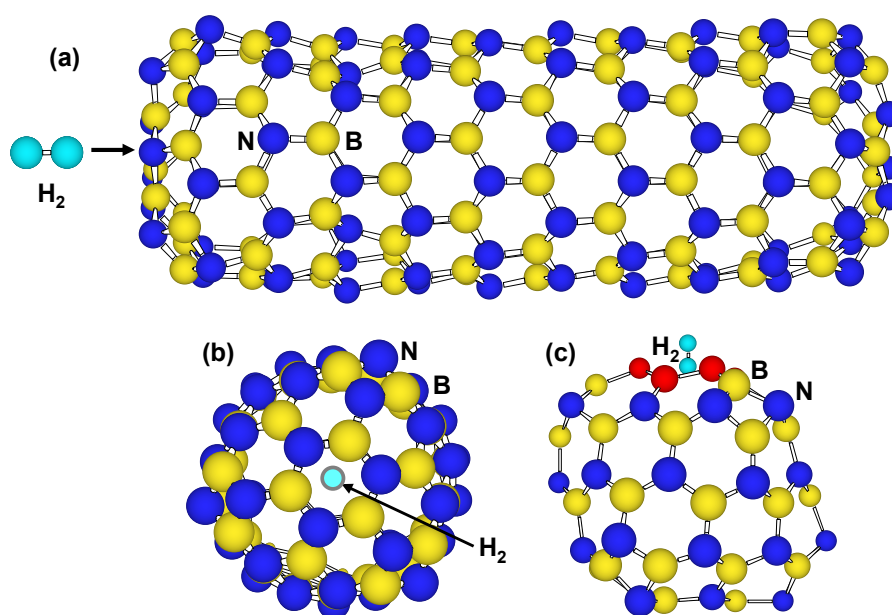
Figure 4. Structure models that H_2 molecule passes through hexagonal BN rings of (**a**,**b**) tip of $B_{99}N_{99}$ nanotube and (**c**) $B_{36}N_{36}$ cluster.

A formation mechanism of BN nanotubes and nanocapsules synthesized in the present work is described below. Metal and boron particles are melted by arc-melting, and during the solidification of the liquid into metal and/or boride nanoparticles, excess boron would react with nitrogen to form BN layers at the surface of the nanoparticles. Because of electrical insulation, BN fullerene materials are usually fabricated by arc-discharge method with specific conducting electrodes such as HfB_2 and ZrB_2. The present arc-melting method from mixed powder has two advantages for BN nanomaterial production. Since the powder becomes conducting by pressing, special electrodes are not needed. In

addition, ordinary, commercial arc-melting furnaces can be used. These advantages indicate a simpler fabrication method compared to the ordinary arc-discharge methods.

Although gas storages of hydrogen and argon in carbon nanotubes have been reported, there are few reports for gas storage in BN fullerene materials and for calculations [21]. Weight increase of the sample in TG measurements was observed as shown in Figure 3. It might be due to the hydrogen gas storage in the BN nanomaterials. Since there would be metal and boron nanoparticles in the separated BN nanomaterials even after the separation, further qualification and evaluation of the samples are needed for hydrogen storage.

Carbon fullerenes and boron nitride fullerenes are sublimed at 600 and 1000 °C, respectively. Boron nitride fullerenes would storage H_2 molecules with smaller energy than carbon fullerenes, and would give good stability at high temperature. Boron nitride fullerene materials would be a better candidate for H_2 storage materials.

3.3. Molecular Orbital Calculations of Hydrogen Storage in Boron Nitride and C Clusters

Figure 5 is a structural model of hydrogen atoms chemisorbed on boron and nitrogen for BN clusters and carbon clusters. Atoms bonded with hydrogen are moved outside from the clusters. Energies for hydrogen chemisorption on each position are summarized as Table 3. Hydrogen bonding with nitrogen is more stable than that with boron, and hydrogen bonding with carbon is more stable than C_{60}. This result indicates the chemical modification of carbon fullerenes. When two hydrogen atoms were chemisorbed on carbon clusters, energies of carbon clusters increased.
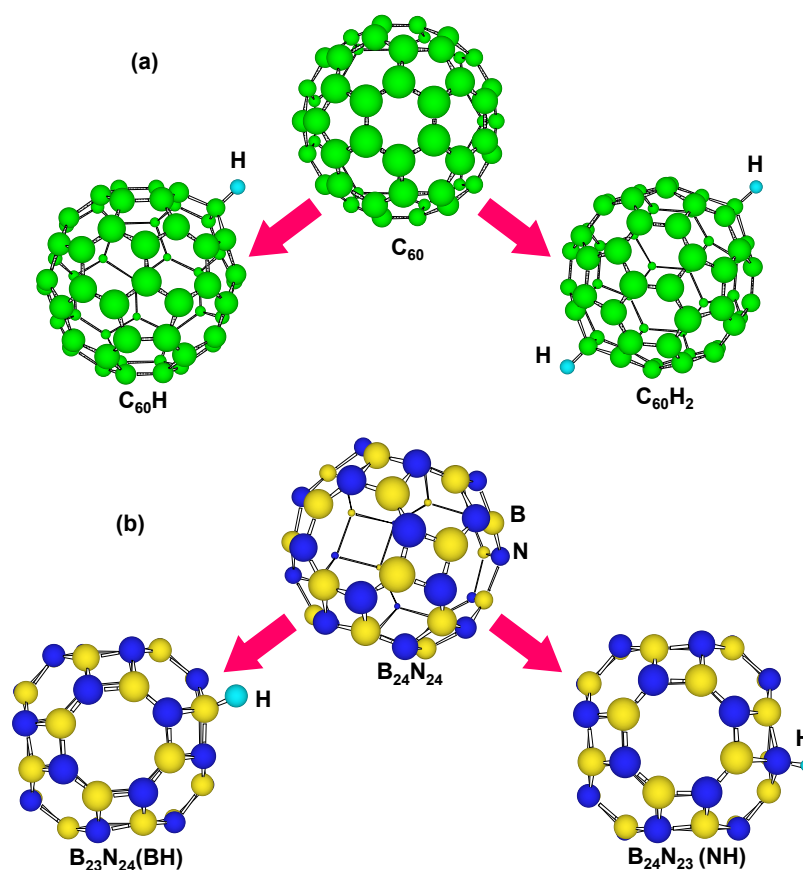

Figure 5. Structural models of H atoms chemisorbed on (**a**) C_{60} and (**b**) $B_{24}N_{24}$.

Table 3. Chemisorption energy of hydrogen (H) atoms on C_{60} and $B_{24}N_{24}$. ΔE = (Heat of formation after hydrogen addition) − (Heat of formation before hydrogen addition).

Cluster	Number of H atoms	Additional position of H	Heat of formation (eV)		ΔE (eV)
			Before addition	**After addition**	
C_{60}	1	C	35.21	35.03	−0.18
	2	C	35.21	35.81	0.6
$B_{24}N_{24}$	1	B	−36.12	−34.66	1.46
	1	N	−36.12	−35.67	0.45
$B_{36}N_{36}$	1	B of tetragonal ring	−69.33	−67.83	1.50
	1	N of tetragonal ring	−69.33	−69.16	0.17
	1	B of tetragonal ring	−69.33	−67.51	1.83
	1	N of tetragonal ring	−69.33	−68.83	0.51

In the calculation, chemisorption of hydrogen was performed on outside of cage, and on boron, nitrogen and carbon of tetragonal and hexagonal rings. The $B_{36}N_{36}$ cluster has tetragonal and hexagonal BN rings, and there are four kinds of boron and nitrogen positions for the hydrogen chemisorption, as shown in Figure 6. For the stability calculations of H_2 molecules in these clusters, 30 H_2 molecules were also introduced in $B_{24}N_{24}$, $B_{36}N_{36}$, $B_{60}N_{60}$ and C_{60}. Figure 5 is a structural model of hydrogen atoms chemisorbed on boron and nitrogen for $B_{36}N_{36}$. Energies for hydrogen chemisorption on each position are summarized as Table 3. Hydrogen bonding with nitrogen is more stable than that with boron because nitrogen atoms are more electrophilic compared to boron atoms. In addition, hydrogen bonding on tetragonal ring is more stable than that of hexagonal ring. Chemisoption of hydrogen with C_{60} reduced the energy. When two hydrogen atoms were chemisorbed on carbon clusters, energies of carbon clusters increased.
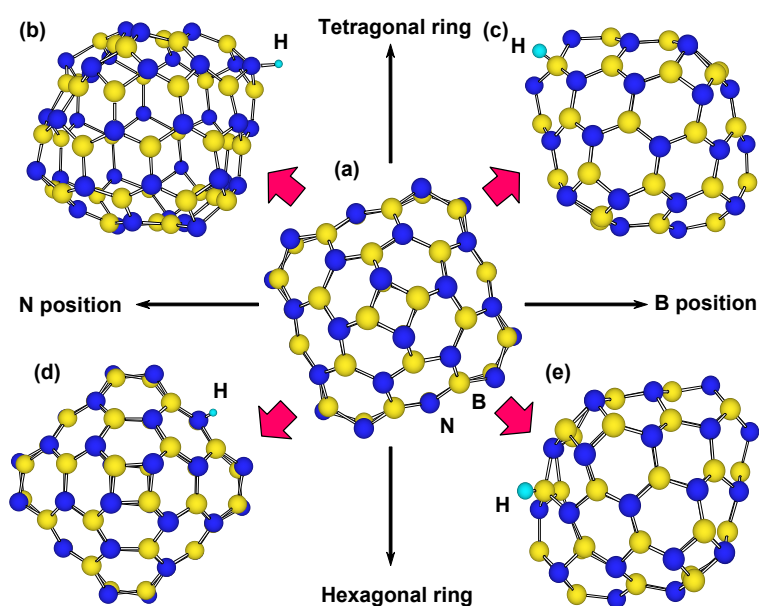

Figure 6. Structure models for hydrogen chemisorption on $B_{36}N_{36}$: (**a**) structural model of $B_{36}N_{36}$; (**b**,**c**) structural models of hydrogen chemisorption on N and B positions of tetragonal BN ring, respectively; and (**d**,**e**) structural models of hydrogen chemisorbed on N and B positions of hexagonal BN ring, respectively.

To investigate stability of H_2 molecules in clusters, energies were calculated for H_2 molecules introduced in the center of clusters. The structural models are shown in Figure 7. Energies of C_{60}, $B_{24}N_{24}$, $B_{36}N_{36}$ and $B_{60}N_{60}$ were calculated to be 0.58, 20.71, 20.93 and 20.82 eV/mol atom, respectively. This result indicates that $B_{24}N_{24}$, $B_{36}N_{36}$ and $B_{60}N_{60}$ with H_2 molecules are more stable than C_{60} with H_2 molecule, and that $B_{36}N_{36}$ is the most stable in BN clusters.
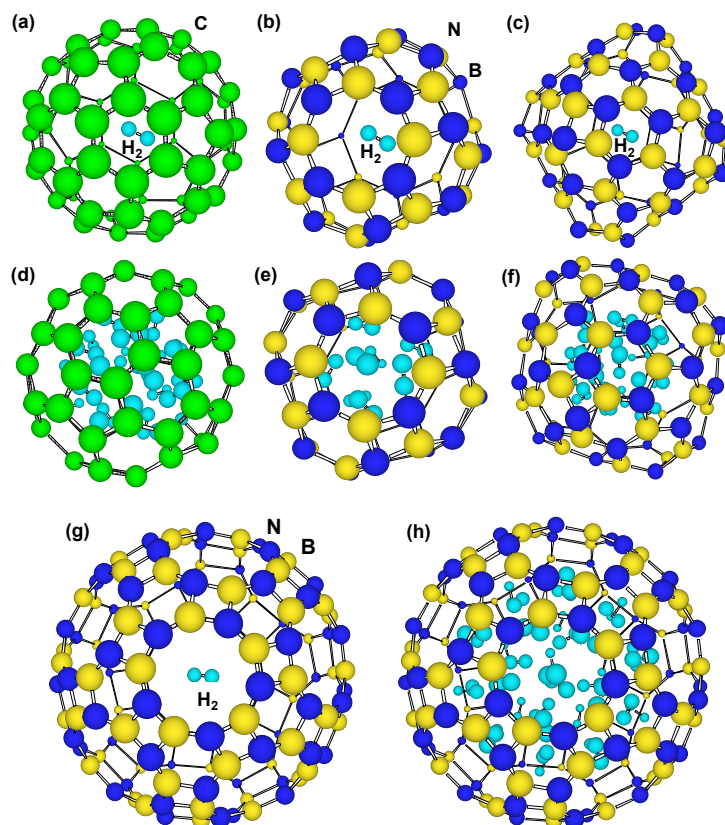
Figure 7. Optimized structural models of H_2 molecules in the clusters. A H_2 molecule in the center of (**a**) C_{60}; (**b**) $B_{24}N_{24}$; (**c**) $B_{36}N_{36}$; (**d**) 22 H_2 molecules inside C_{60} and 8 atoms chemisorbed; (**e**) 9 H_2 molecules in $B_{24}N_{24}$; and (**f**) 20 molecules in $B_{36}N_{36}$; (**g**) 1 and (**h**) 38 H_2 molecules in $B_{60}N_{60}$.

Hydrogen storage (wt%) of $B_{60}N_{60}$ cluster was calculated, and structural models are shown in Figure 7. Other C_{60}, $B_{24}N_{24}$ and $B_{36}N_{36}$ were calculated, as summarized in Table 4. From Table 4, C and BN cluster showed possibility of hydrogen storage of ~6.5 and ~4.9 wt%, respectively.

Although hydrogen storage (wt%) of C_{60} is better than those of BN clusters, energy increase by hydrogen addition is higher for C_{60} (4.6–5.2 eV/H atom) compared to BN clusters (1.0–3.1 eV/H atom), which would be due to C–H interaction. This indicates that needed energy for hydrogen storage in BN clusters is lower compared to the C_{60}. From Table 4, stability of H_2 molecules in $B_{24}N_{24}$ and $B_{36}N_{36}$ seems to be higher than that of C_{60}. Hydrogen atoms were calculated to be chemisorbed inside C_{60}, as shown in Table 4. This indicates that inside of C_{60} also has good reactivity as well as outside of the cage. Chemisorption inside the C_{60} clusters may indicate that hydrogen capacity may gradually reduce under the adsorption-desorption cycles. On the other hand, BN clusters have no chemisorption inside the clusters, which indicates that the BN clusters would be a better candidate for stable adsorption-desorption

cycles. C_{60} cluster shows the minimum energies in spite of the positive values. It is believed that p-electrons outside and inside of the cage would increase the energy. However, s-electrons in the 5- and 6-membered carbon rings would stabilize the cage structure. Hydrogen addition to the C_{60} decreased the energy, which agrees with the above description. The hydrogen storage of the present BN cluster was calculated to be ~4.9 wt%, and the measured values were 1–3 wt%. This might be due to the remained catalytic metals in the sample, which reduces the storage ratio.

Table 4. Energy of clusters with hydrogen.

Cluster	Introduced H_2	Heat of formation (eV)	H atoms chemisorbed inside cluster	Hydrogen storage (wt%)	Heat of formation per added H atom (eV/H atom)
C_{60}	0	35.21	0	5.8–6.5	4.9–5.2
	22	143.01	0		
	25	164.87	4		
	26	169.63	8 *		
$B_{24}N_{24}$	0	−36.12	0	2.9	3.0
	9	−9.44	0		
$B_{36}N_{36}$	0	−69.33	0	4.3	3.1
	20	−6.66	0		
$B_{60}N_{60}$	0	−100.28	0	4.9	1.0
	38	−61.74	0		

* A C–C bond was broken.

Although carbon nanotubes are oxidized at ~600 °C, BN nanomaterials are almost stable ~900 °C in air, which indicates BN fullerenes have higher thermal and chemical stability than those of carbon fullerenes. BN fullerenes with good thermal and chemical stability can store H_2 molecules with less energy, and they have the same chemisorption energy and higher stability, compared to carbon clusters. BN fullerene materials would be better candidates for H_2 storage materials.

3.4. Effects of Endohedral Element in $B_{24}N_{24}$ Clusters on Hydrogenation

Figure 8 is a structural model of hydrogen atoms chemisorbed on nitrogen position for $M@B_{24}N_{24}$. Energies for hydrogen chemisorption on boron and nitrogen positions are summarized as Table 5. Heats of formation (eV) of $M@B_{24}N_{24}$ by hydrogenation are indicated in Figure 9. In Table 5 and Figure 9, "None" means that metal catalyst was not encaged in $B_{24}N_{24}$, and "BH" and "NH" means that hydrogen atom was chemisorbed on boron and nitrogen, respectively. Figure 9 shows that hydrogen bonding with nitrogen is more stable than that with boron because nitrogen atoms are more electrophilic compared to boron atoms. Figure 9 also indicates that energies of chemisorption on $M@B_{24}N_{24}$ are much lower than that of $B_{24}N_{24}$. From this result, Li atom works as a good endohedral element for hydrogen chemisorption. Metal catalysts in the present work have been reported to generate hydrides such as LiH because of strong interaction between hydrogen and metal atoms. In the present work, it is clarified that Li doping and nitrogen positions are suitable for hydrogenation for the $B_{24}N_{24}$ clusters.
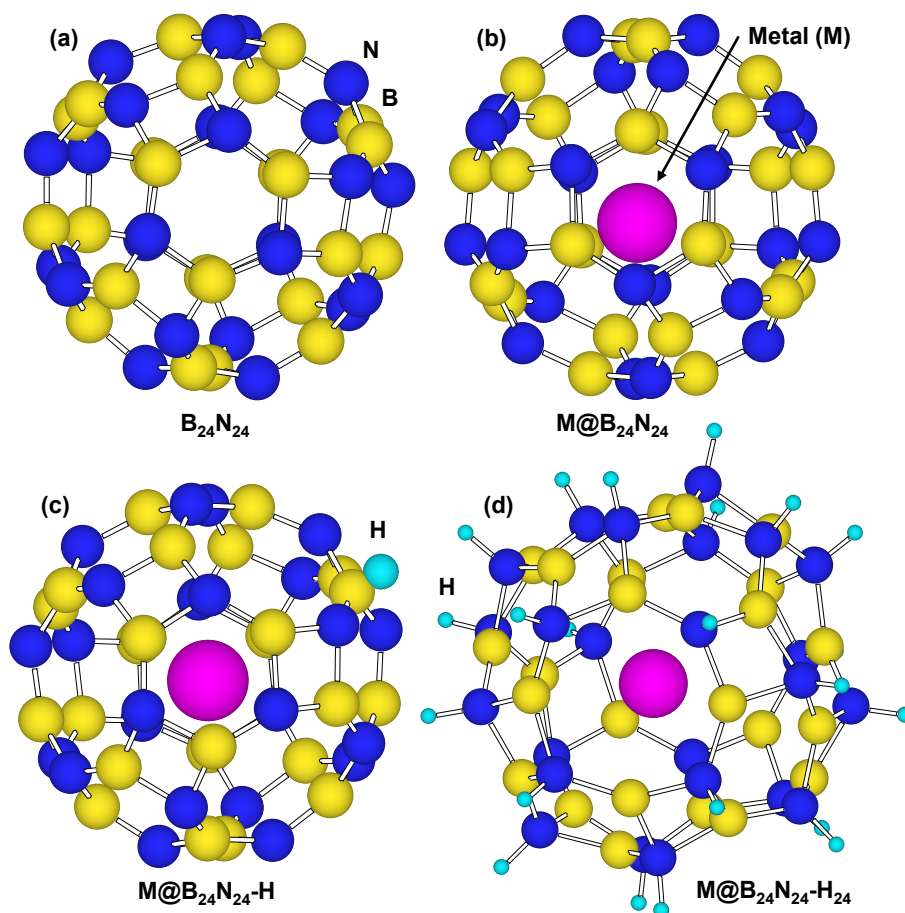
Figure 8. Structural models for (**a**) B₂₄N₂₄; (**b**) endohedral M@B₂₄N₂₄; (**c**) hydrogenated M@B₂₄N₂₄-H; and (**d**) M@B₂₄N₂₄ which chemisorbed 24 hydrogen atoms.

Table 5. Chemisorption energies of a hydrogen atom on M@B₂₄N₂₄.

Cluster	Hydrogenation position	Heat of formation (eV)	ΔE * (eV)
$B_{24}N_{24}$	Un-hydrogenated	−36.12	0
	B	−34.66	1.46
	N	−35.67	0.45
$Li@B_{24}N_{24}$	Un-hydrogenated	−36.79	0
	B	−37.96	−1.17
	N	−38.05	−1.26
$Na@B_{24}N_{24}$	Un-hydrogenated	−35.38	0
	B	−36.43	−1.05
	N	−36.62	−1.24
$K@B_{24}N_{24}$	Un-hydrogenated	−31.80	0
	B	−32.84	−1.04
	N	−32.90	−1.10

* ΔE = (heat of formation after hydrogen addition) − (heat of formation before hydrogen addition).
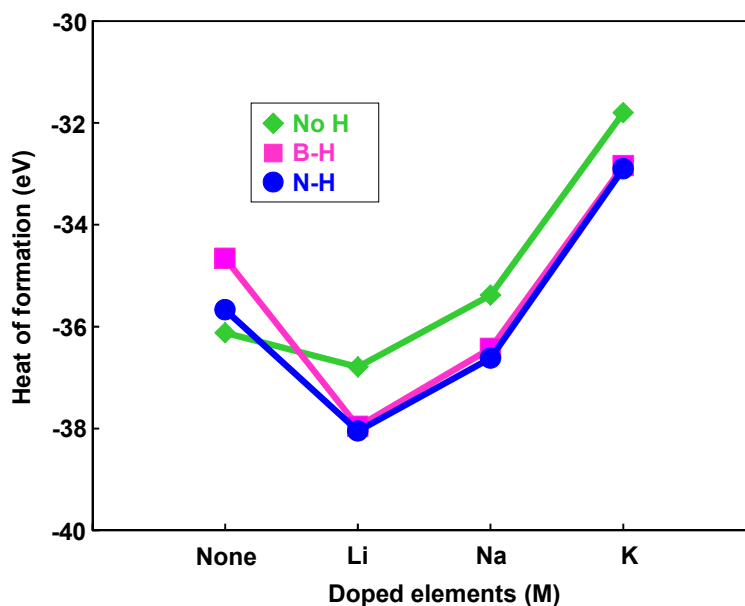
Figure 9. Heats of formation of hydrogenation for $M@B_{24}N_{24}$ clusters by endohedral elements.

Bond lengths of B–H and N–H for $M@B_{24}N_{24}$ are summarized in Table 6. B–H and N–H distance decreased by doping element in the BN cluster. Bond lengths of N–H are shorter than that of B–H for these BN clusters, and the bond length of N–H for $Li@B_{24}N_{24}$ is the shortest. The endohedral atoms appear to decrease the repulsion energy between the electrons of the hydrogen atom and the p-electrons of $B_{24}N_{24}$. Figure 8d is a structural model of $M@B_{24}N_{24}H_{24}$, which indicates hydrogenation on all nitrogen positions for $M@B_{24}N_{24}$, and the hydrogen storage capacity is summarized in Table 7. Li is also a good element for hydrogen storage capacity because Li is the lightest element of these. Energy levels and density of states for $B_{24}N_{24}$ and $Li@B_{24}N_{24}$ are shown in Figure 10. Fermi levels in energy level diagrams and DOS diagrams correspond to 0 eV. $B_{24}N_{24}$ and $Li@B_{24}N_{24}$ show energy gaps of 4.8873 and 0.0247 eV between the highest occupied molecular orbital (HOMO) and the lowest unoccupied molecular orbital (LUMO), respectively. This means that electron of Li element transferred to the $B_{24}N_{24}$ cage, and electronic state of BN cluster would change from semiconductor to metallic property by Li doping in BN clusters.

Table 6. Bond length of B–H and N–H on $M@B_{24}N_{24}$.

Cluster	B–H (Å)	N–H (Å)
$B_{24}N_{24}$	1.229	1.010
$Li@B_{24}N_{24}$	0.695	0.616
$Na@B_{24}N_{24}$	1.203	1.005
$K@B_{24}N_{24}$	1.204	1.006

Table 7. Hydrogen storage capacity of chemisorption on nitrogen position of $M@B_{24}N_{24}$.

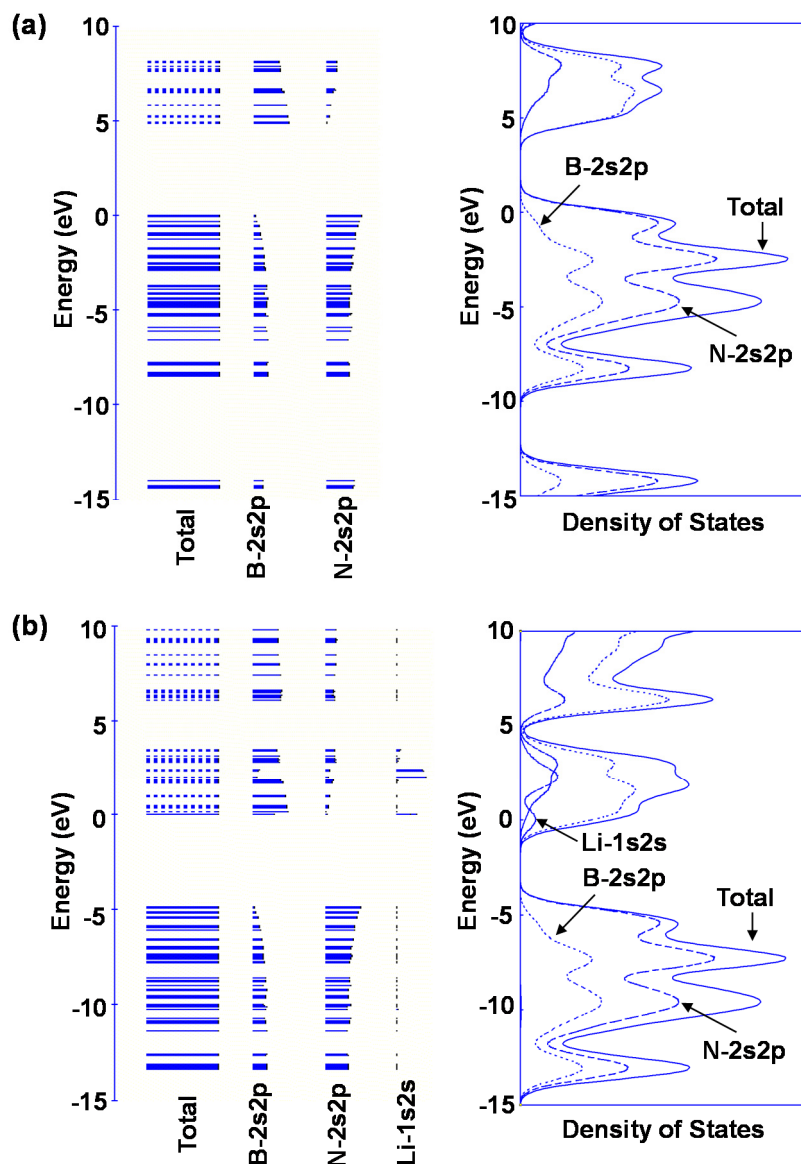| Cluster	Hydrogen storage (wt%)
$Li@B_{24}N_{24}H_{24}$	3.86
$Na@B_{24}N_{24}H_{24}$	3.76
$K@B_{24}N_{24}H_{24}$	3.67

Figure 10. Energy levels diagrams and density of states of (**a**) $B_{24}N_{24}$ and (**b**) $Li@B_{24}N_{24}$.

Although it was reported that BN nanotubes were produced by lithium vapor, synthesis of Li@BN has not been reported yet. BN fullerenes have high thermal and chemical stability, and M@BN fullerenes have lower energy of chemisorption compared to the present work. Since the BN clusters were reported to be doped with metal elements, M@BN clusters would be produced. BN fullerene materials with endohedral element such as Li would be better candidates for H_2 storage materials.

3.5. Molecular Dynamics Calculations of Hydrogen Storage in C$_{60}$ Clusters

C_{60} included a H_2 molecule kept in stable state at $T = 298$ K and $P = 0.1$ MPa. This unit cell is shown in Figure 11. This model was calculated with $N = 62$ atoms, $T = 298$ K and $P = 0.1$ MPa. Although the H_2 molecule vibrated in the C_{60} cage, it was not discharged from the cage. Some H_2 molecules were stored in the C_{60} cage when the pressure was 5 MPa. This unit cell is shown in Figure 12, which is composed of 32 C_{60} (*fcc*) with 288 H_2 molecules (*fcc*). This model was calculated with $N = 2496$ atoms and $P = 5$ MPa. H_2 molecules pass through the hexagonal rings of the C_{60} cage at 0.5 ps.
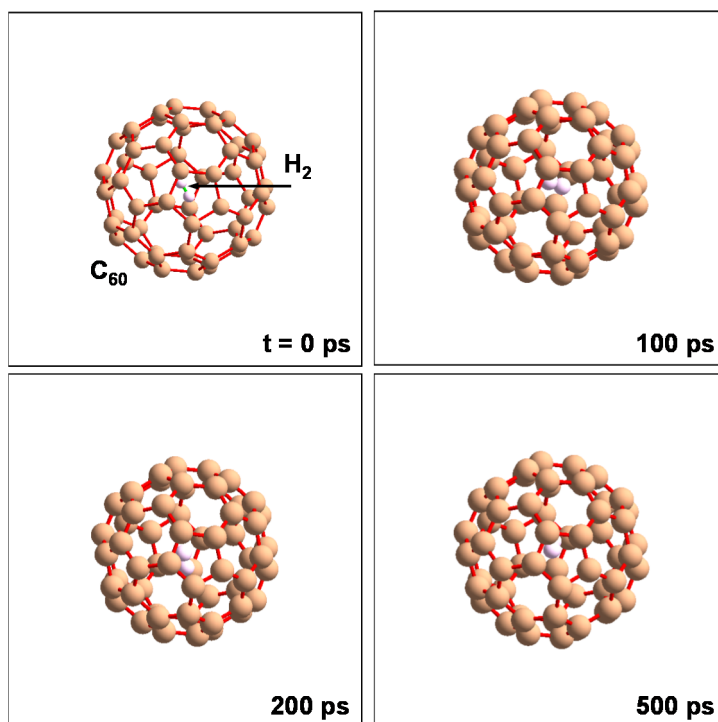
Figure 11. Molecular dynamics calculation to confirm stability of H_2 molecule into C_{60} at 298 K and 105 Pa. NTP ensembles and organic potential were used in the calculation.
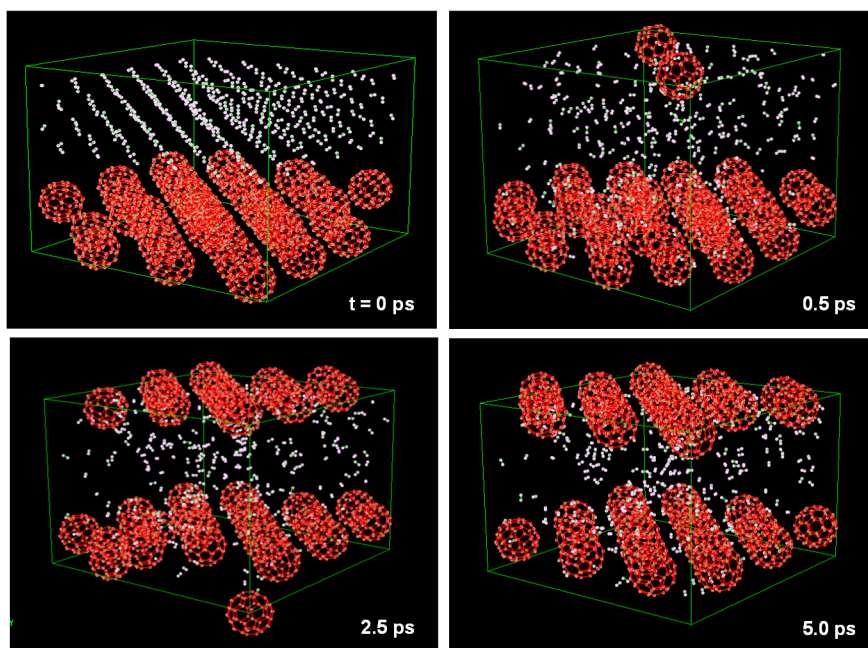

Figure 12. Molecular dynamics calculation to find condition of H_2 gas storage. Unit cell is composed from 32 C_{60} (*fcc*) with 288 H_2 molecules (*fcc*). NPH ensembles and organic potential were used in the calculation.

After introducing H_2 molecules into the C_{60} cage at 2.5 ps, they are stored and stable in C_{60}. Figure 13 shows a schematic model of a single H_2 molecule stored in a hexagonal ring of C_{60}. These results indicate that fullerene-like materials can store H_2 gas in cage at $T = 298$ K and $P = 0.1$ MPa, and some H_2 molecules were stored in the C_{60} cage when the pressure was greater than 5 MPa. It is known that

H_2 molecules are adsorbed on the walls of single-walled carbon nanotubes over 7 MPa as an experimental result [26]. Since a C_{60} cluster has a large curvature and H_2 molecules are very small compared to C_{60}, it is considered that adsorption and storage of H_2 gas occur at the same time. Detailed theoretical calculation on hydrogen storage in BN nanomaterials has also been performed [27–31].
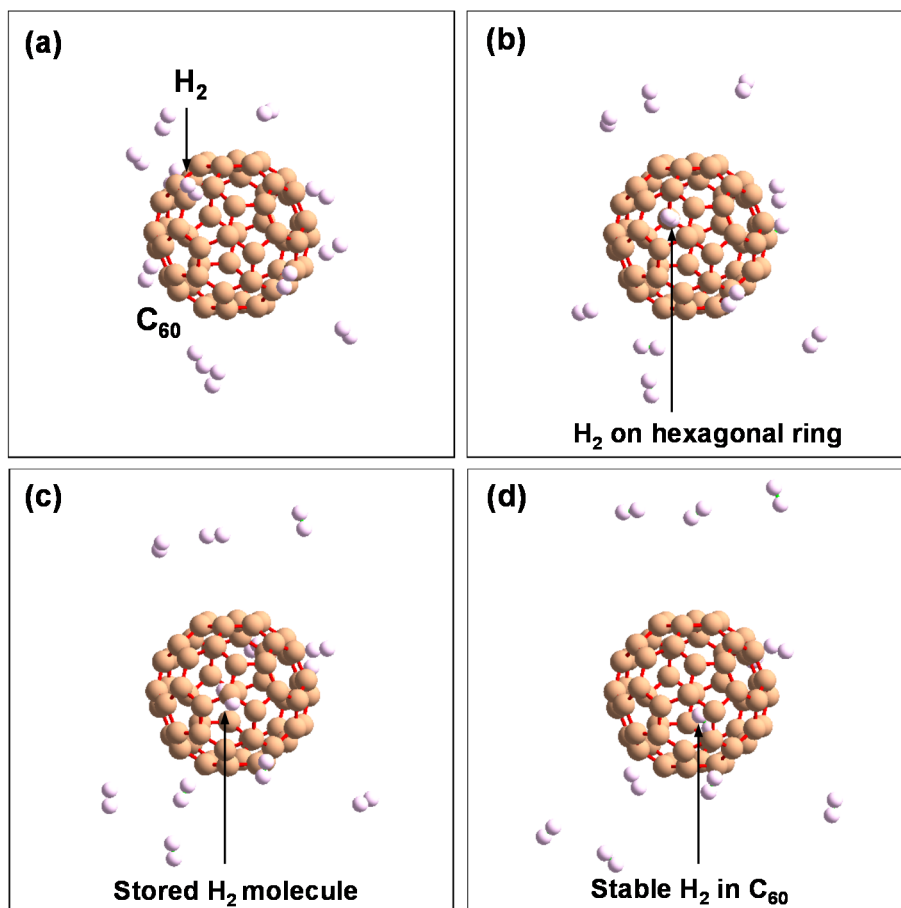

Figure 13. Schematic model of H_2 molecule stored in hexagonal ring in the order of (**a**–**d**).

4. Conclusions

HREM observation showed the formation of BN nanotubes, nanocapsules and nanocages, which were synthesized from mixtures of LaB_6, Pd, and boron powder by using an arc melting method. Although samples produced with Pd include only BN nanocapsule structures, samples produced with LaB_6 present BN nanocapsule, nanotube and nanocage structures. After separation of BN nanomaterials using ethanol, hydrogen storage was measured by TG/DTA, and the BN nanomaterials produced from LaB_6 and Pd/boron powder showed possibility of hydrogen storage of ~3 wt%. Energies for BN and C clusters with hydrogen were investigated by molecular orbital calculations. Stabilities of these clusters were estimated from the energies, and possibility of H_2 storage ability was predicted by these results. $B_{24}N_{24}$, $B_{36}N_{36}$, $B_{60}N_{60}$ and C_{60} clusters were selected as the tip structure of the nanotubes. Chemisorption calculation of hydrogen for BN clusters showed that hydrogen bonding with nitrogen atoms was more stable than that with boron atoms, and that hydrogen bonding with tetragonal ring is more stable than that with hexagonal ring. Energy increase by hydrogen addition to C_{60} is higher compared to BN clusters because of C–H interaction, which indicates that the BN clusters

have higher stability with hydrogen atoms. BN cluster and C cluster showed possibility of H_2 storage of ~4.9 wt% and ~6.5 wt%, respectively. H_2 storage of C cluster is better than those of BN clusters. However, stability of H_2 molecules in BN clusters might be higher than that of C clusters. Energies of hydrogenation for $B_{24}N_{24}$ were also investigated by molecular orbital calculations. Chemisorption calculation of hydrogen in the $B_{24}N_{24}$ clusters showed that hydrogen bonding with nitrogen atoms was more stable than that with boron atoms. Chemisorption calculations also indicate that endohedral elements decreased energies of hydrogenation and Li atom is suitable element for hydrogen chemisorption. Molecular dynamics calculations showed that a single H_2 molecule remains in a stable state in a C_{60} cage at $T = 298$ K and $P = 0.1$ MPa. It is confirmed that pressure of over 5 MPa is required to store H_2 molecules in a C_{60} cage. As a result of SPE calculations, H_2 molecules enter from hexagonal rings of fullerene-like materials. The energy required of H_2 discharge from fullerene-like materials is similar to that of H_2 storage. The present study indicates that BN fullerene materials could be a one of the possible candidates as hydrogen gas storage materials.

Acknowledgments

Conflicts of Interest

The author declares no conflict of interest.

References

1. Schlapbach, L.; Züttel, A. Hydrogen-storage materials for mobile applications. *Nature* **2001**, *414*, 353–358.
2. Dillon, A.C.; Jones, K.M.; Bekkedahl, T.A.; Kiang, H.; Bethune, D.S.; Heben, M.J. Storage of hydrogen in single-walled carbon nanotubes. *Nature* **1997**, *386*, 377–379.
3. Chen, P.; Wu, X.; Lin, J.; Tan, K.L. High H_2 uptake by alkali-doped carbon nanotubes under ambient pressure and moderate temperatures. *Science* **1999**, *285*, 91–93.
4. Dujardin, E.; Ebbesen, T.W.; Hiura, H.; Tanigaki, K. Capillarity and wetting of carbon nanotubes. *Science* **1994**, *265*, 1850–1852.
5. Liu, C.; Fan, Y.Y.; Liu, M.; Cong, H.T.; Cheng, H.M.; Dresselhaus, M.S. Hydrogen storage in single-walled carbon nanotubes at room temperature. *Science* **1999**, *286*, 1127–1129.
6. Nützenadel, C.; Züttel, A.; Chartouni, D.; Schlapbach, L. Electrochemical storage of hydrogen in nanotube materials. *Electrochem. Solid-State Lett.* **1999**, *2*, 30–32.
7. Wu, X.B.; Chen, P.; Lin, J.; Tan, K.L. Hydrogen uptake by carbon nanotubes. *Int. J. Hydrog. Energy* **2000**, *25*, 261–265.
8. Oku, T.; Narita, I.; Koi, N.; Nishiwaki, A.; Suganuma, K.; Inoue, M.; Hiraga, K.; Matsuda, T.; Hirabayashi, M.; Tokoro, H.; *et al.* Boron Nitride Nanocage Clusters, Nanotubes, Nanohorns, Nanoparticles, and Nanocapsules. In *B-C-N Nanotubes and Related Nanostructures*; Yap, Y.K., Ed.; Springer: Berlin, Germany, 2009; pp. 149–194.

9. Moussa, G.; Demirci, U.B.; Malo, S.; Bernard, S.; Mielea, P. Hollow core@mesoporous shell boron nitride nanopolyhedron-confined ammonia borane: A pure B–N–H composite for chemical hydrogen storage. *J. Mater. Chem. A* **2014**, *2*, 7717–7722.

10. Weng, Q.; Wang, X.; Bando, Y.; Golberg, D. One-step template-free synthesis of highly porous boron nitride microsponges for hydrogen storage. *Adv. Energy Mater.* **2014**, *4*, doi:10.1002/aenm.201301525.

11. Moussa, G.; Salameh, C.; Bruma, A.; Malo, S.; Demirci, U.B.; Bernard, S.; Miele, P. Nanostructured boron nitride: From molecular design to hydrogen storage application. *Inorganics* **2014**, *2*, 396–409.

12. Liu, Y.; Liu, W.; Wang, R.; Hao, L.; Jiao, W. Hydrogen storage using Na-decorated graphyne and its boron nitride analog. *Int. J. Hydrog. Energy* **2014**, *39*, 12757–12764.

13. Lei, W.; Zhang, H.; Wu, Y.; Zhang, B.; Liua, D.; Qin, S.; Liu, Z.; Liu, L.; Ma, Y.; Chen, Y.; *et al*. Oxygen-doped boron nitride nanosheets with excellent performance in hydrogen storage. *Nano Energy* **2014**, *6*, 219–224.

14. Ebrahimi-Nejad, S.; Shokuhfar, A. Compressive buckling of open-ended boron nitride nanotubes in hydrogen storage applications. *Phys. E* **2013**, *50*, 29–36.

15. Wang, Y.; Wang, F.; Xu, B.; Zhang, J.; Sun, Q.; Jia, Y. Theoretical prediction of hydrogen storage on Li-decorated boron nitride atomic chains. *J. Appl. Phys.* **2013**, *113*, 064309:1–064309:6.

16. Lim, S.H.; Luo, J.; Ji, W.; Lin, J. Synthesis of boron nitride nanotubes and its hydrogen uptake. *Catal. Today* **2007**, *120*, 346–350.

17. Oku, T. Direct structure analysis of advanced nanomaterials by high-resolution electron microscopy. *Nanotechnol. Rev.* **2012**, *1*, 389–425.

18. Oku, T. High-resolution electron microscopy and electron diffraction of perovskite-type superconducting copper oxides. *Nanotechnol. Rev.* **2014**, *3*, 413–444.

19. Oku, T.; Nishiwaki, A.; Narita, I.; Gonda, M. Formation and structure of $B_{24}N_{24}$ clusters. *Chem. Phys. Lett.* **2003**, *380*, 620–623.

20. Koi, N.; Oku, T.; Narita, I.; Suganuma, K. Synthesis of huge boron nitride cages. *Diam. Relat. Mater.* **2005**, *14*, 1190–1192.

21. Oku, T.; Kuno, M.; Narita, I. Hydrogen storage in boron nitride nanomaterials studied by TG/DTA and cluster calculation. *J. Phys. Chem. Solids* **2004**, *65*, 549–552.

22. Oku, T.; Narita, I. Calculation of H_2 gas storage for boron nitride and carbon nanotubes studied from the cluster calculation. *Phys. B* **2002**, *323*, 216–218.

23. Koi, N.; Oku, T. Hydrogen storage in boron nitride and carbon clusters studied by molecular orbital calculations. *Solid State Commun.* **2004**, *131*, 121–124.

24. Koi, N.; Oku, T.; Suganuma, K. Effects of endohedral element in $B_{24}N_{24}$ clusters on hydrogenation studied by molecular orbital calculations. *Phys. E* **2005**, *29*, 541–545.

25. Oku, T.; Narita, I.; Nishiwaki, A.; Koi, N.; Suganuma, K.; Hatakeyama, R.; Hirata, T.; Tokoro, H.; Fujii, S. Formation, atomic structures and properties of carbon nanocage materials. *Top. Appl. Phys.* **2006**, *100*, 187–216.

26. Ye, Y.; Ahn, C.C.; Witham, C.; Fultz, B.; Liu, J.; Rinzler, A.G.; Colbert, D.; Smith, K.A.; Smalley, R.E. Hydrogen adsorption and cohesive energy of single-walled carbon nanotubes. *Appl. Phys. Lett.* **1999**, *74*, 2307–2309.

27. Sun, Q.; Wang, Q.; Jena, P. Storage of molecular hydrogen in B-N cage: Energetics and thermal stability. *Nano Lett.* **2005**, *5*, 1273–1277.

28. Zhou, Z.; Zhao, J.; Chen, Z.; Gao, X.; Yan, T.; Wen, B.; Schleyer, P.R. Comparative study of hydrogen adsorption on carbon and BN nanotubes. *J. Phys. Chem. B* **2006**, *110*, 13363–13369.

29. Wu, H.; Fan, X.; Kuo, J.L. Metal free hydrogenation reaction on carbon doped boron nitride fullerene: A DFT study on the kinetic issue. *Int. J. Hydrog. Energy* **2012**, *37*, 14336–14342.

30. Wen, S.H.; Deng, W.Q.; Han, K.L. Endohedral BN metallofullerene $M@B_{36}N_{36}$ complex as promising hydrogen storage materials. *J. Phys. Chem. C* **2008**, *112*, 12195–12200.

31. Venkataramanan, N.S.; Belosludov, R.V.; Note, R.; Sahara, R.; Mizuseki, H.; Kawazoe, Y. Theoretical investigation on the alkali-metal doped BN fullerene as a material for hydrogen storage. *Chem. Phys.* **2010**, *377*, 54–59.